

AD-A235 025



TION PAGE

Form Approved  
OMB No. 0704-0188

Page 1 hour air release, including the date for removing instructions, searching existing data sources, the collection of information. Send comments regarding this burden estimate or any other aspect of this Washington Headquarters Service, Directorate for Information Operations and Reports, 1215 Jefferson Management and Budget, Paperwork Reduction Project (0704-0188), Washington, DC 20503.

PRW P

1. AGENCY USE ONLY (Leave blank)		3. REPORT TYPE AND DATES COVERED FINAL 01 Aug 90 TO 31 Mar 91	
4. TITLE AND SUBTITLE Superconducting High TC Thin Film Vortex-Flow Transistor		5. FUNDING NUMBERS SDIO 1602	
6. AUTHOR(S) Dr Hohenwarter		8. PERFORMING ORGANIZATION REPORT NUMBER AFOSR-TP-91-0300	
7. PERFORMING ORGANIZATION NAME(S) AND ADDRESS(ES) Hypress, Inc 500 Executive Blvd Elmsford, NY 10523		10. SPONSORING/MONITORING AGENCY REPORT NUMBER F49620-90-C-0054	
9. SPONSORING/MONITORING AGENCY NAME(S) AND ADDRESS(ES) AFOSR/NE Bldg 410 Bolling AFB Washington DC 20332-6448 Dr. Harold Weinstock		11. SUPPLEMENTARY NOTES	
12a. DISTRIBUTION/AVAILABILITY STATEMENT APPROVED FOR PUBLIC RELEASE: DISTRIBUTION IS UNLIMITED		12b. DISTRIBUTION CODE	
13. ABSTRACT (Maximum 200 words) Hypres, Inc. has investigated a device based on vortex-flow in a superconducting thin-film. This transistor-like device is referred to as a superconducting flux-flow transistor (SFFT). Alongside step edge and grain boundary tunneling junctions the SFFT appears to be a promising candidate for active high temperature circuits. SFFT operation relies on the control of electrical characteristics at the output terminals by a magnetic field at the device boundaries. This field can be provided by the flow of a current in a control line; the device's input resistance hence will be very low. Substantial power gain can result. The low input resistance, yet moderate output resistant of the device appears beneficial for interfacing digital Josephson junction electronics with semiconductor circuits. This was proven in an experiment where Josephson junction was connected to a SFFT.			
14. SUBJECT TERMS		15. NUMBER OF PAGES	
		16. PRICE CODE	
17. SECURITY CLASSIFICATION OF REPORT UNCLASSIFIED	18. SECURITY CLASSIFICATION OF THIS PAGE UNCLASSIFIED	19. SECURITY CLASSIFICATION OF ABSTRACT UNCLASSIFIED	20. LIMITATION OF ABSTRACT UNLIMITED

## GENERAL INSTRUCTIONS FOR COMPLETING SF 298

The Report Documentation Page (RDP) is used in announcing and cataloging reports. It is important that this information be consistent with the rest of the report, particularly the cover and title page. Instructions for filling in each block of the form follow. It is important to *stay within the lines* to meet optical scanning requirements.

**Block 1. Agency Use Only (Leave blank).**

**Block 2. Report Date.** Full publication date including day, month, and year, if available (e.g. 1 Jan 88). Must cite at least the year.

**Block 3. Type of Report and Dates Covered.** State whether report is interim, final, etc. If applicable, enter inclusive report dates (e.g. 10 Jun 87 - 30 Jun 88).

**Block 4. Title and Subtitle.** A title is taken from the part of the report that provides the most meaningful and complete information. When a report is prepared in more than one volume, repeat the primary title, add volume number, and include subtitle for the specific volume. On classified documents enter the title classification in parentheses.

**Block 5. Funding Numbers.** To include contract and grant numbers; may include program element number(s), project number(s), task number(s), and work unit number(s). Use the following labels:

C - Contract	PR - Project
G - Grant	TA - Task
PE - Program Element	WU - Work Unit Accession No.

**Block 6. Author(s).** Name(s) of person(s) responsible for writing the report, performing the research, or credited with the content of the report. If editor or compiler, this should follow the name(s).

**Block 7. Performing Organization Name(s) and Address(es).** Self-explanatory.

**Block 8. Performing Organization Report Number.** Enter the unique alphanumeric report number(s) assigned by the organization performing the report.

**Block 9. Sponsoring/Monitoring Agency Name(s) and Address(es).** Self-explanatory.

**Block 10. Sponsoring/Monitoring Agency Report Number.** (If known)

**Block 11. Supplementary Notes.** Enter information not included elsewhere such as: Prepared in cooperation with..., Trans. of..., To be published in.... When a report is revised, include a statement whether the new report supersedes or supplements the older report.

**Block 12a. Distribution/Availability Statement.** Denotes public availability or limitations. Cite any availability to the public. Enter additional limitations or special markings in all capitals (e.g. NOFORN, REL, ITAR).

DOD - See DoDD 5230.24, "Distribution Statements on Technical Documents."

DOE - See authorities.

NASA - See Handbook NHB 2200.2.

NTIS - Leave blank.

**Block 12b. Distribution Code.**

DOD - Leave blank.

DOE - Enter DOE distribution categories from the Standard Distribution for Unclassified Scientific and Technical Reports.

NASA - Leave blank.

NTIS - Leave blank.

**Block 13. Abstract.** Include a brief (*Maximum 200 words*) factual summary of the most significant information contained in the report.

**Block 14. Subject Terms.** Keywords or phrases identifying major subjects in the report.

**Block 15. Number of Pages.** Enter the total number of pages.

**Block 16. Price Code.** Enter appropriate price code (*NTIS only*).

**Blocks 17. - 19. Security Classifications.** Self-explanatory. Enter U.S. Security Classification in accordance with U.S. Security Regulations (i.e., UNCLASSIFIED). If form contains classified information, stamp classification on the top and bottom of the page.

**Block 20. Limitation of Abstract.** This block must be completed to assign a limitation to the abstract. Enter either UL (unlimited) or SAR (same as report). An entry in this block is necessary if the abstract is to be limited. If blank, the abstract is assumed to be unlimited.

Final Report for the Phase I Project

Superconducting High T<sub>c</sub> Thin Film Vortex-Flow Transistor

Topic Number: SDIO 90-015

Contract Number: F49620-90-C-0054

Submitted by:

G.K.G. Hohenwarter



March 28, 1991

Accession For	
NTIS GSA&I	<input checked="" type="checkbox"/>
DTIC TAB	<input type="checkbox"/>
Unannounced	<input type="checkbox"/>
Justification	
By _____	
Distribution/	
Availability Codes	
Dist	Avail and/or Special
A-1	

Table of Contents

1.	Summary	p. 2
2.	Flux Flow Transistor operating principles	p. 3
3.	Mask design for device fabrication	p. 6
4.	Device fabrication	p. 9
5.	Device testing	p.11
6.	Electrical characteristics	p.13
7.	Equivalent circuit	p.17
8.	SFFT line driver	p.19 -
9.	Device stability	p.21
10.	SFFT applications	p.22
11.	Conclusions	p.25
12.	References	p.26

## Superconducting High T<sub>c</sub> Thin-Film Vortex-Flow Transistor

### 1. SUMMARY

HYPRES, Inc. has investigated a device based on vortex-flow in a superconducting thin-film. This transistor-like device is referred to as a superconducting flux-flow transistor (SFFT). Alongside step edge and grain boundary tunneling junctions the SFFT appears to be a promising candidate for active high temperature circuits. SFFT operation relies on the control of electrical characteristics at the output terminals by a magnetic field at the device boundaries. This field can be provided by the flow of a current in a control line; the device's input resistance hence will be very low. Substantial power gain can result. The low input resistance, yet moderate output resistance of the device appears beneficial for interfacing digital Josephson junction electronics with semiconductor circuits. This was proven in an experiment where a Josephson junction was connected to a SFFT.

A mask set for evaluation of fabrication issues and device functionality plus integratability into a digital low temperature circuit system was designed and fabricated. Films of YBCO and NbN superconductors were used for evaluation of the concept. Processes for tuning of device parameters were developed. Models for parasitic elements, transresistance and output parameters were established and verified. Additional potential SFFT applications

were identified. It was successfully demonstrated that the SFFT possesses power gain, non-linear inductance plus low input impedance and moderate output impedance levels.

Work performed under this contract was complemented by efforts of the University of Wisconsin, Madison and Sandia National Laboratories, Albuquerque, NM.

## 2. Flux Flow Transistor Operating Principles

The philosophy behind the flux flow transistor is to control the flow of vortices in thin superconducting films. A superconducting thin film with a magnetic field applied perpendicular to it can enter a state where this flux is admitted into the film in quantized units, so-called vortices [1]. If a current flows through the film, these vortices will be subject to an accelerating force similar to a Lorentz force. The resulting motion causes a small voltage to appear across the vortex core (Fig. 1).

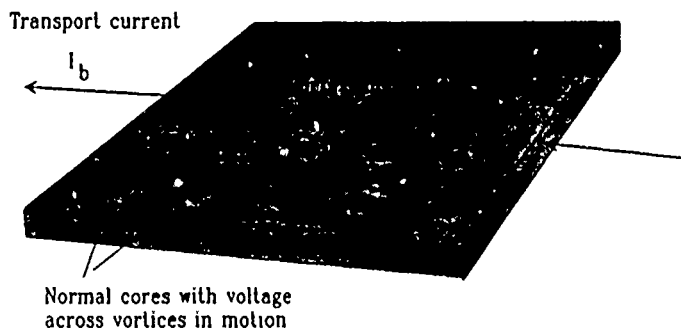


Fig. 1 Vortex motion in a thin superconducting film

Vortex drift velocity is low due to resistive loss (viscous

flow). This speed limiting factor and the low sensitivity of the flow mechanism to external magnetic field led to the exploration of parallel variable thickness bridges instead of a continuous film [2] (Fig. 2).

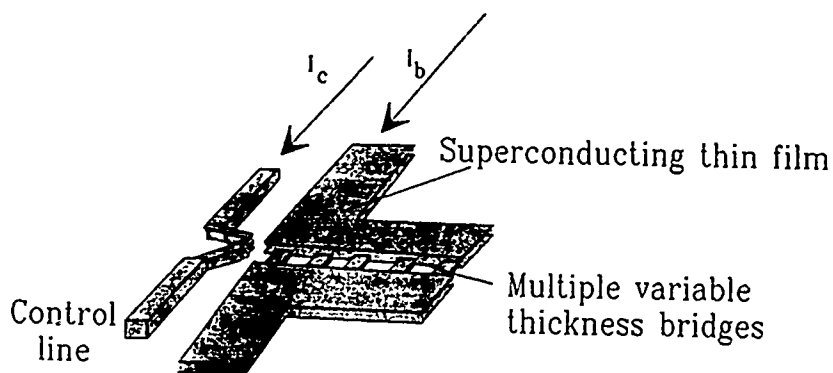


Fig. 2 Single layer flux flow transistor

The arrangement of multiple parallel links increases sensitivity to magnetic field and decreases transit time in the structure. If an increasing current  $I_b$  is driven through this device, its current-voltage curve will initially display a supercurrent without any voltage across the links. As current increases, so does the magnetic self-field at the device boundaries. A voltage appears at the device terminals once this field becomes large enough to nucleate vortices in the film (point A, Fig. 3).

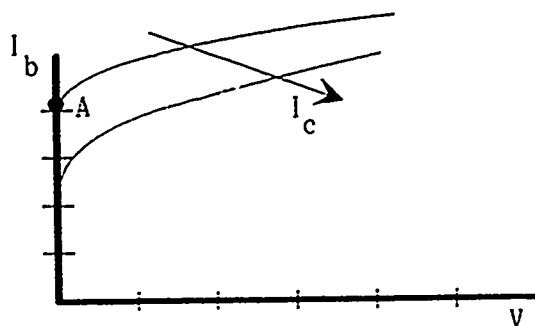


Fig. 3 Idealized I-V characteristic of a SFFT

Under these conditions magnetic vortices have entered the link region and are flowing through it. This was demonstrated in an experiment where two SFFTs were brought into close contact. One device was driven into the flux flow state. In the other, unbiased device, this resulted in a voltage across the output [2] (Giaver's dc transformer experiment).

The observed resistive state in the I-V curve of an SFFT can easily be influenced by an applied magnetic field. Therefore, a three or four terminal device results, if a control line is placed close to the link region (see Fig. 2).

A resistive state has previously been observed in so-called thin-film cryotrons [3], referred to as a foot. In that device, designed for switching between two states, this effect was generally considered undesirable, however, since it hampered operation by reducing the gain when the device was to be switched into the normal state.



### 3. Mask design for device fabrication

Masks for photolithographic device patterning were made from Kodak high resolution negative plates (2"x 2"). To achieve a minimal feature size with the available setup, double reductions were employed. In this process, the first step was to develop a high resolution plate with the device features enlarged by the reduction factor of the process. This high resolution plate was then combined with a conventional, full size transparency to become the original for the final mask (Fig. 4).

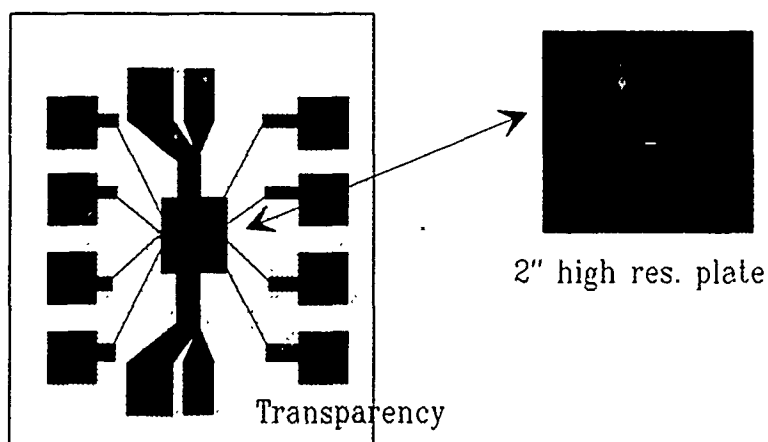


Fig. 4 Double step mask reduction

With this technique, devices with feature sizes as small as 5  $\mu\text{m}$  were fabricated. Several masks sets were produced in this manner to evaluate various aspects of device operation. A representative layout for a SFFT with a 50 Ohm coplanar slotline at its in- and outputs is shown in Fig. 5.

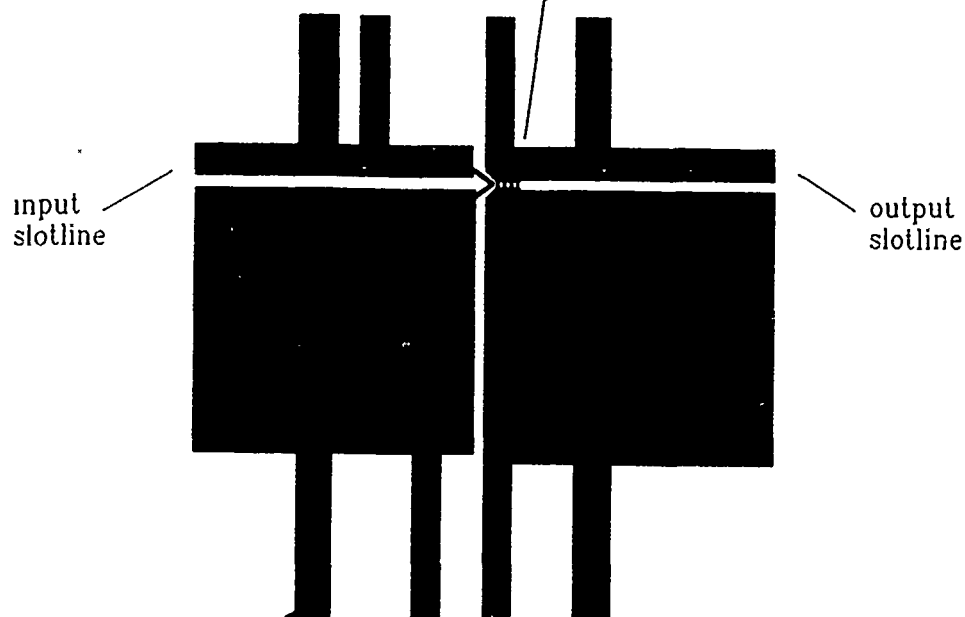


Fig. 5 Mask layout for SFFT fabrication

Only the basic layout is shown here since black and white reproductions do not easily lead to multi-level displays of the mask design. SFFT link length and width were chosen to be 10  $\mu\text{m}$ , the hole width was 15  $\mu\text{m}$ . The coplanar slotline gap width of 30  $\mu\text{m}$  in conjunction with a line width of 75  $\mu\text{m}$  yielded a characteristic impedance close to 50 Ohms. Dimensions were the result of computations which assumed this configuration to be equivalent to one half of a coplanar line (center conductor with two groundplanes separated by gaps). Commercial software (EESof Linecalc) was then used to calculate the dimensions of a coplanar line with half the characteristic impedance of the slotline.

The SFFT consisted of four individual links located between ground and the slotline conductor. Dimensions chosen were the results of several experiments toward optimization of device parameters. It was found, for example, that any number of links

larger than about four does not contribute to an increased transresistance of the device. Also, device gain is maximized by minimizing the distance between the control line and device body.

For experiments with line driver circuits, the mask set was modified to contain areas in which Josephson junctions and resistors could be added (Fig. 6).

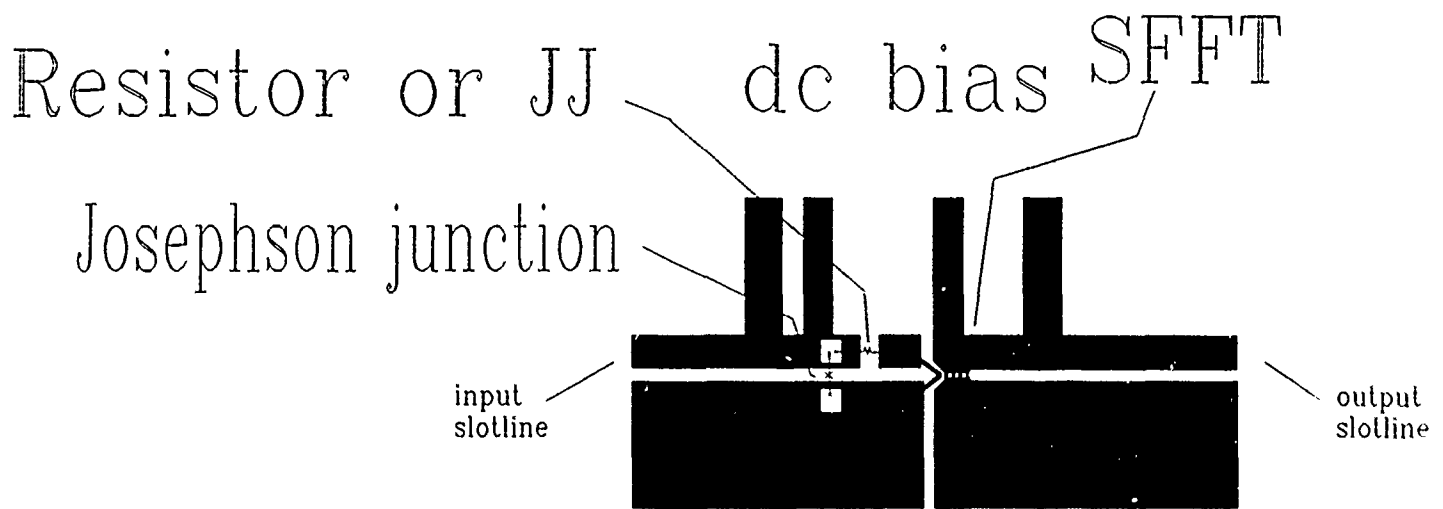


Fig. 6 Josephson junction driven SFFT mask layout

Once again, only the basic design (lowest level) is shown, with the location of junctions and resistors indicated in the figure. Here, the input slotline is connected to ground through a Josephson junction. It also leads to the SFFT control line through either a Josephson junction or a resistor. The SFFT output configuration remained unchanged.

#### 4. Device fabrication

SFFT's were fabricated using both niobium nitride (NbN) and yttrium barium copper oxide (YBCO) thin films. NbN films were magnetron sputter deposited to 75 nm thickness on fused quartz substrates with 10 mil thickness [4]. Patterning with AZ 4330 positive photoresist spun at about 3000 rpm for 30 seconds and subsequent reactive ion etching defined the first film layer features. In the next process step, photoresist was again applied and the region of the variable thickness bridges was opened to allow for tuning of the device. Waycot HR 100 negative resist (4000 rpm, 15 sec) was employed in this step. Tuning occurred via anodization at low voltages in a bath of sodium tetraborate and boric acid (3.4 g and 2.7 g, respectively, for 500 ml of water). While limiting the current into the sample with a large series resistor (1 MOhm) voltages of up to 70 V were used in this process. Samples were subjected to a short curing time of approximately 1 minute to allow for equalization of oxide thickness in all areas of the device.

YBCO films with a thickness of 300 nm were fabricated by multilayer deposition on  $\text{LaAlO}_3$  substrates with subsequent anneal at 820 degrees Celsius [5]. This process yielded films with a current density of approximately  $3 \times 10^5 \text{ A/cm}^2$  at 77 K. Susceptibility measurements showed transition temperatures of around 87 K with a run to run variability of about 1 K. The rf surface resistance of some of the fabricated films was determined by measurements of the quality factor of a cylindrical cavity with a resonance frequency of 34 GHz. The best films used here demonstrated approximately 7 mOhms surface resistance at 8 GHz

(square law dependence of surface resistance on frequency was assumed).

Films were processed with several different methods. Initially, wet etching with nitric acid was pursued. Patterning was performed with a 3% solution, tuning occurred in a 0.3% nitric acid bath. It was found that this technique yielded unsatisfactory results regarding repeatability of device parameters. Hence, a non-water based etchant (bromine etch) was also considered. At the same time, the patterning process was converted to HR 100 negative photoresist to avoid all exposure of the YBCO films to water. Sample fabrication remained problematic, however, due to deterioration of the photo-resist in the etch bath. Etch rates observed with this process were so low that more than 10 min of exposure to the etchant were required for patterning of a 300 nm film. Possible off-stoichiometry of the films was suspected to contribute to this low rate [6].

Experiments with SFFT's driven by low temperature Josephson junctions were carried out by using high  $T_c$  YBCO films on  $\text{LaAlO}_3$  substrates (20 mil thickness). After YBCO film patterning and device tuning, a niobium film (250 nm) was deposited by dc magnetron sputtering. Patterning followed the same steps as those for NbN films (reactive ion etching). A native oxide barrier was grown via rf plasma discharge. Evaporation of lead (500 nm thickness) formed the counterelectrode. Low value resistors were formed by a dc magnetron sputtered aluminum film of approximately 400 nm thickness. Adhesion and edge coverage problems occurred in this step. Both the Pb and the Al films were patterned by wet

etching. Sample passivation was available via a thin layer of HR 100 photoresist, which did not crack or disintegrate during cycling to 4.2 K.

### 5. Device testing

SFFT devices had to be tuned to achieve the desired resistive state with flux flow in the link region. This tuning was an interactive process that required gradual removal of superconducting film material in the link region. Device characteristics had to be verified after each step. A simple waferprober with a cold stage was therefore constructed. It consisted of an Electroglas Model 131 probe station with a custom built array of so-called pogo pins. This array could be brought into contact with the sample, which was immersed in liquid nitrogen. Thus, rapid sample testing at 77 K became possible.

To verify device operation at elevated frequencies, a simple test fixture consisting of a slab of G 10 epoxy (1/8 " thick) with pogo pins inserted in a pattern corresponding to that of the test masks was used. While precision rf measurements were found to suffer from repeatability problems within the pogo pins, the performance of this fixture yielded nevertheless satisfactory results for the intended purposes. A plot of input reflection coefficient vs. frequency (Fig. 7) for an open input demonstrates a reasonably flat response except for a resonance at about 3.1 GHz, caused by the pogo pin array.

S<sub>11</sub>/M log MAG  
REF 3.0 dB  
2.0 dB/

12

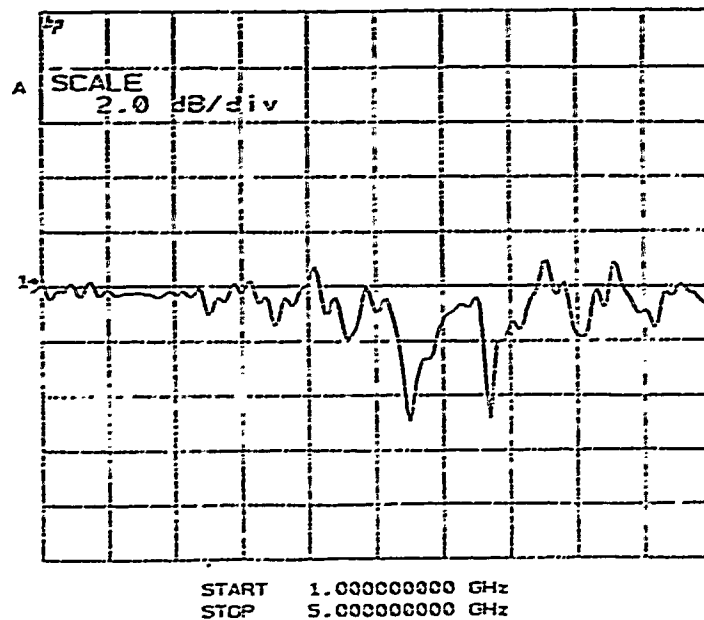


Fig. 7 Input reflection coefficient of rf test fixture  
as a function of frequency

SFFT devices requiring 4.2 K cooling were tested by immersion cooling with liquid helium in a glass dewar. Line lengths between the network analyzer and the device under test were kept to a minimum by utilizing a single wall glass dewar (Pope Scientific, 0.5 l). This arrangement allowed for about an hour of experimentation without requiring refilling.

## 6. Electrical characteristics

YBCO film based SFFTs displayed voltages of up to 30 mV in the flux flow state. NbN devices testing, however, revealed that any

resistive states observed yielded only small voltages on the order of about 10 to 20  $\mu\text{V}$ . Also, YBCO SFFT's displayed transresistances of several Ohms (output voltage swing divided by input current required to achieve that voltage swing); NbN devices showed little magnetic field sensitivity, presumably due to flux pinning in the super-conductor. The following graphs illustrate the progress toward device fabrication and characterization (Figs. 8 and 9):

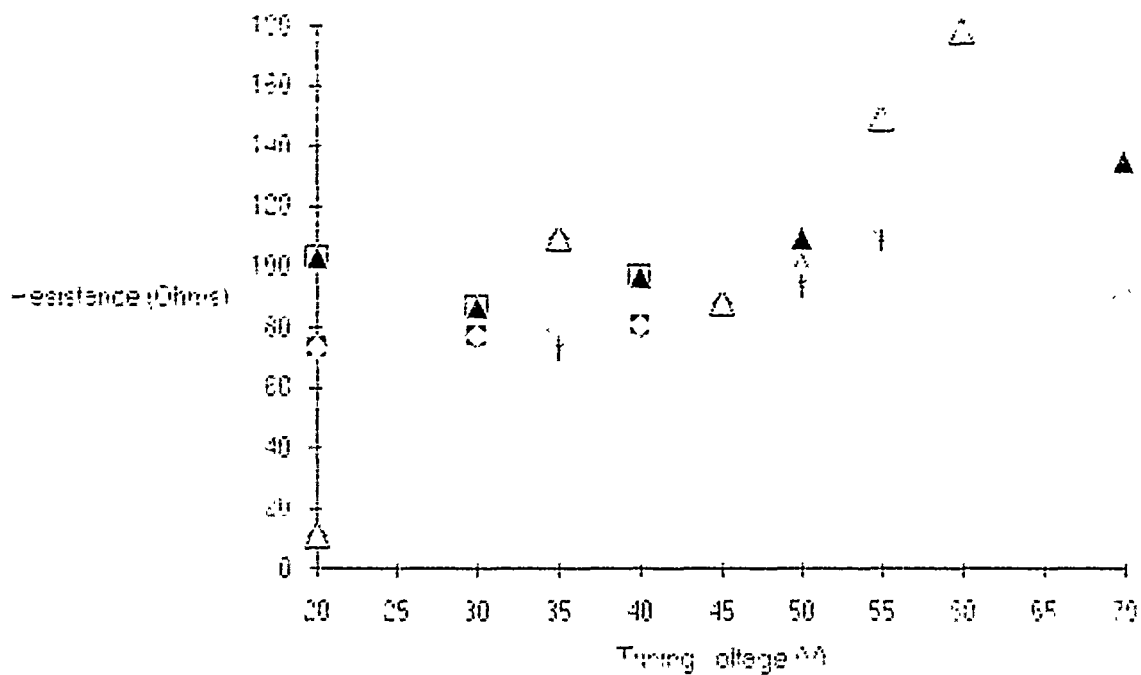


Fig. 8 A Normal state resistance  
as a function of tuning voltage for NbN SFFT's



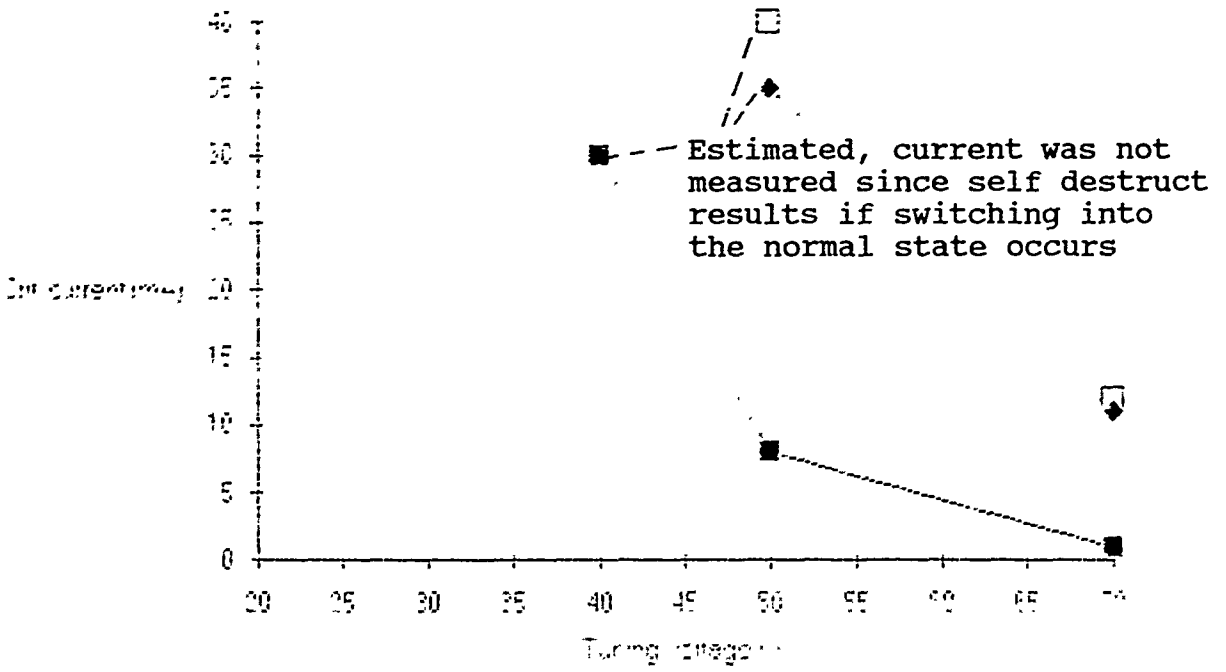


Fig. 8 B Critical current

as a function of tuning voltage for NbN SFTTs

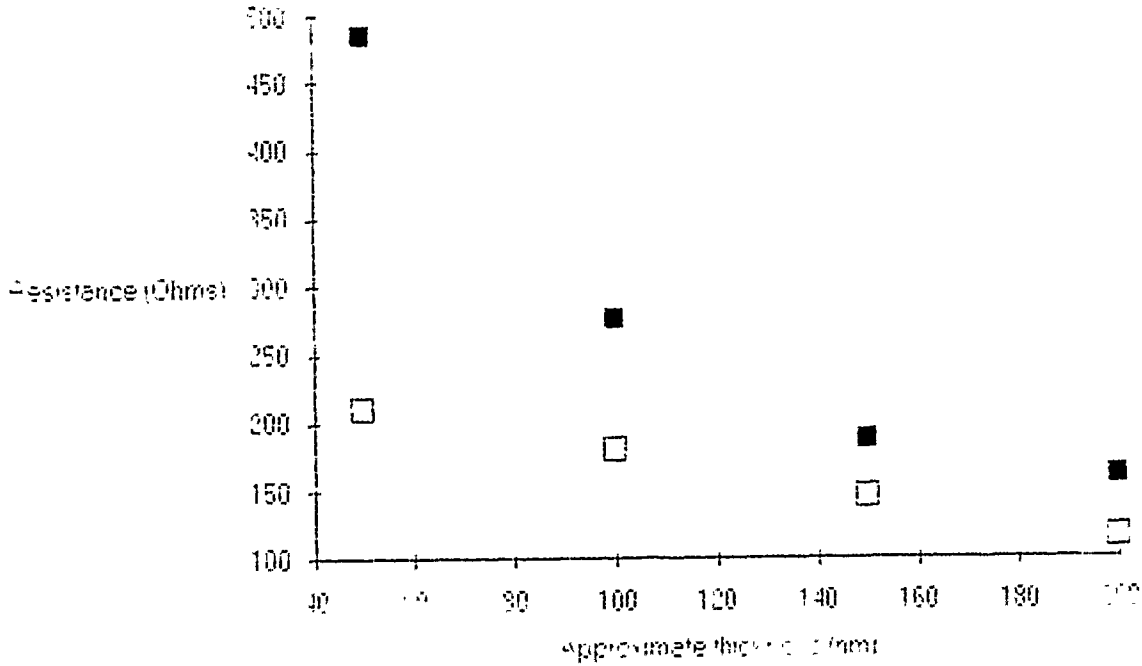


Fig. 9 A Normal state resistance

as a function of thickness for YBCO SFTTs

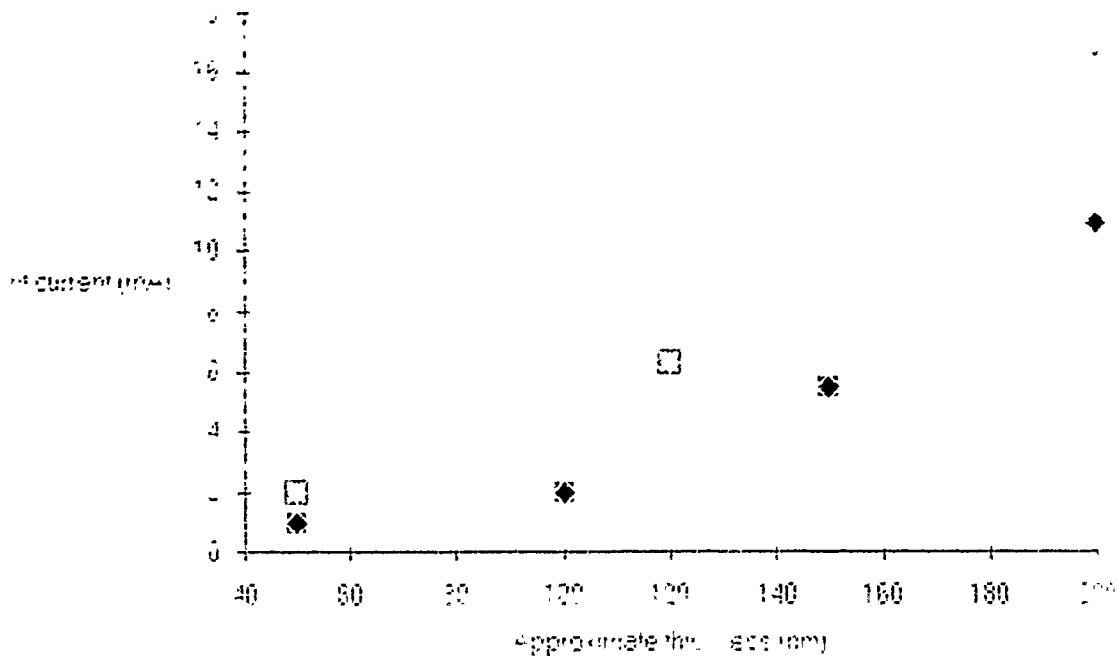


Fig. 9 B Critical current  
as a function of thickness for YBCO SFTTs

These graphs show the normal state resistance (measured at room temperature) and the critical current as a function of the tuning voltage applied during the anodization (thickness) of the NbN (YBCO) films in the link region. Critical current decreases and normal state resistance increases as the links are tuned to smaller and smaller thickness. Data on YBCO critical current dependency are sparse due to fabrication difficulties. The level of involvement necessary for extensive process development was beyond the scope of this work. Exploration of these relationships which may well prove useful for repeated controllable device fabrication hence had to be deferred.

As previously mentioned, NbN devices did not exhibit any

significant voltages past a level of about 20  $\mu\text{V}$ . Hence, no device characteristic is offered here. Several YBCO devices did show encouraging results. The best measured I-V characteristic of a YBCO device shows the dependence of the resistive state on current  $I_c$  flowing through the control line (Fig. 10).

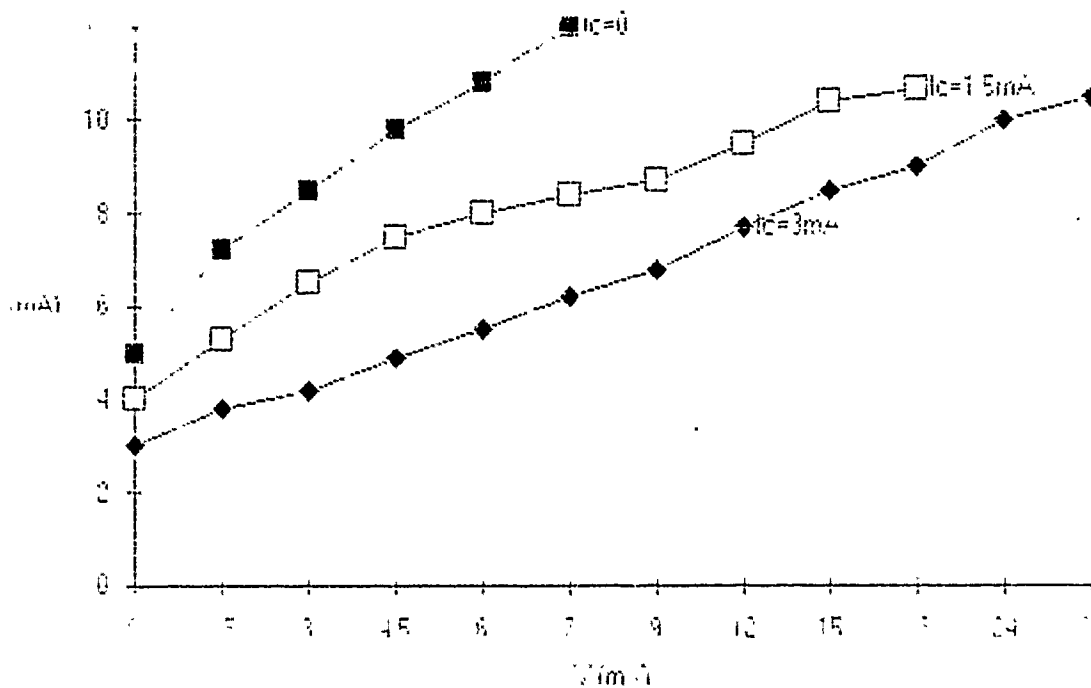


Fig. 10 SFFT I-V curve

The transresistance of this device ( $dV_{out}/dI_{control}$ ) was 2 Ohms at  $V = 6$  mV and  $I_c = 1.5$  mA and its output resistance 2.5 Ohms. Definition of a dc voltage gain is not meaningful; for high frequency applications this can be done and both frequency dependent voltage and power gain result. Current gain was about .8. Parameters were measured at 77 K.

Determination of device switching speed was attempted early on by establishing evidence of the SFFT's capability to function as an

oscillator [7]. The highest observed frequency of operation was achieved by a ring resonator stabilized YBCO device with a 7.5 GHz oscillating frequency [8]. While it has been claimed that SFFT's can achieve transit frequencies in excess of 50 GHz, proof for this is not yet available. Some explanation of device function is offered by the simple concept of Abrikosov vortex motion in a superconducting film [9]. Discrepancies remain, however with respect to anticipated device speed vs. experimentally established evidence of fast device response. After all, the propagation velocity of Abrikosov vortices is so low (on the order of  $3 \times 10^3$  m/s) that GHz operation should not be possible. Yet it has been observed and documented. The influence of grain boundary tunneling on device behavior has not at all been pursued yet. Especially in YBCO films with their well established weak link type grain boundaries of micrometer size the ultimate determination of device operating principles has not been reached conclusively. Only a more comprehensive, systematic approach will answer some of these questions.

The section of SFFT line driver operation will provide some of the experimental results relevant to this work.

### 7. Equivalent circuit

The unique characteristics of the SFFT are reflected in the devices' electrical equivalent circuit (Fig. 11, parameters were determined with an HP 8510 network analyzer).

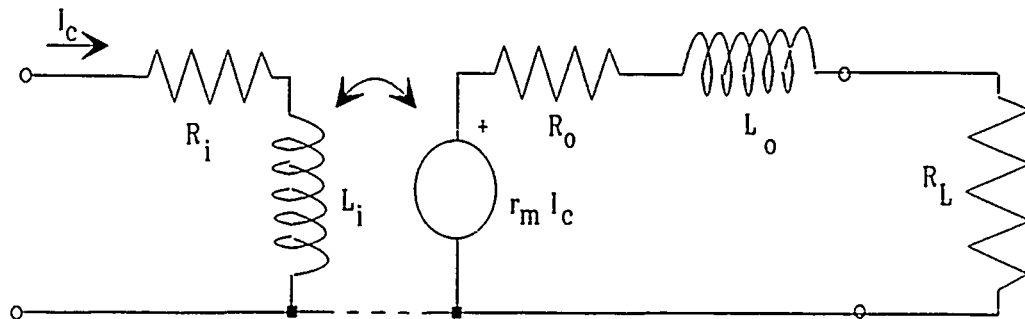


Fig. 11. Electrical equivalent circuit of the SFFT

The superconducting input line of the SFFT represents a short with a small inductance associated with it. This small inductance is difficult to measure in the presence of discontinuities from transmission line interfaces. A device layout as shown in the section on mask design exhibited an input inductance of approximately 50 pH. Loss in the superconductor at rf frequencies was found to be best modeled by a small series resistor on the order of several milliOhms [9]. The characteristics at the SFFTs output were more amenable to direct measurement. The superconductor in the multiple link region is weakened and thus possesses a measurable inductance and resistance. Devices with

four links were found to possess output inductances of several hundred pH and an output resistance of a few Ohms, dependent on the link thickness tuning and dc current bias. While these nonlinearities may be of use in parametric amplifier applications, for example, this was not pursued further.

### 8. SFFT line driver

Superconducting Flux Flow Transistors appear to possess nearly ideal characteristics for applications in interface circuits between relatively high current, low impedance, low temperature Josephson electronic circuits and low current, high impedance semiconductor devices. The SFFT's low input impedance permits a substantial current to be driven through it from a low temperature Josephson junction. An equivalent circuit of such an arrangement is shown in Fig. 12.

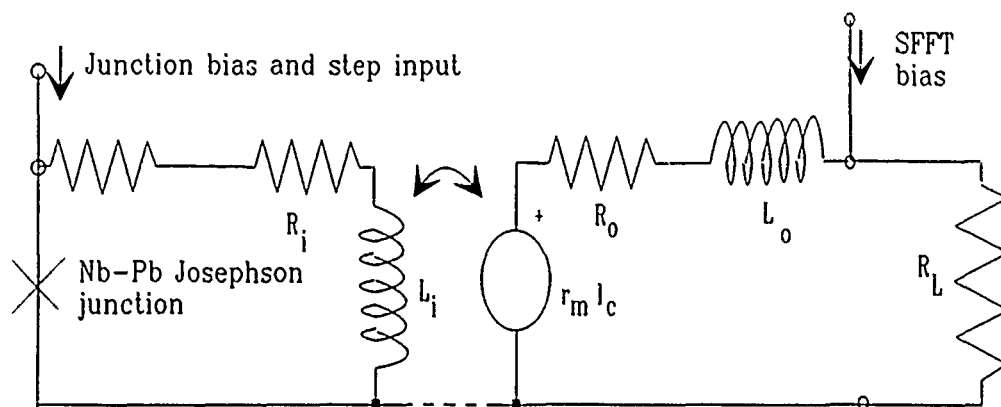


Fig. 12 Equivalent circuit of a Josephson junction driving a SFFT

Here the slotline coming from the input was fed into a Nb-Pb Josephson junction connected to the ground plane (see section on mask design). Connection to the input of the SFFT was established by a resistor. At a junction size of  $40 \times 40 \mu\text{m}$  and a critical current density of  $500 \text{ A/cm}^2$  sufficient critical current (8 mA) resulted to drive the SFFT through a resistor with a value of roughly 1 Ohm. The transresistance of the SFFT the results in an output voltage swing that can be substantially larger than that of a single low temperature Josephson junction. Several devices were fabricated with YBCO SFFTs driven by a Nb-Pb Josephson tunnel junction. Success was limited due to adhesion and step coverage problems. In a related experiment with a Tl based film, however, success was achieved and the concept was demonstrated [10]. In this experiment, the tunnel junction was fed with a step signal derived from a Tektronix S-12 sampling unit with a S-52 step generator. The output from the SFFT was then fed to a sampling head (S-6) in the S-12 unit. A recorded trace of output voltage is shown in Fig. 13.

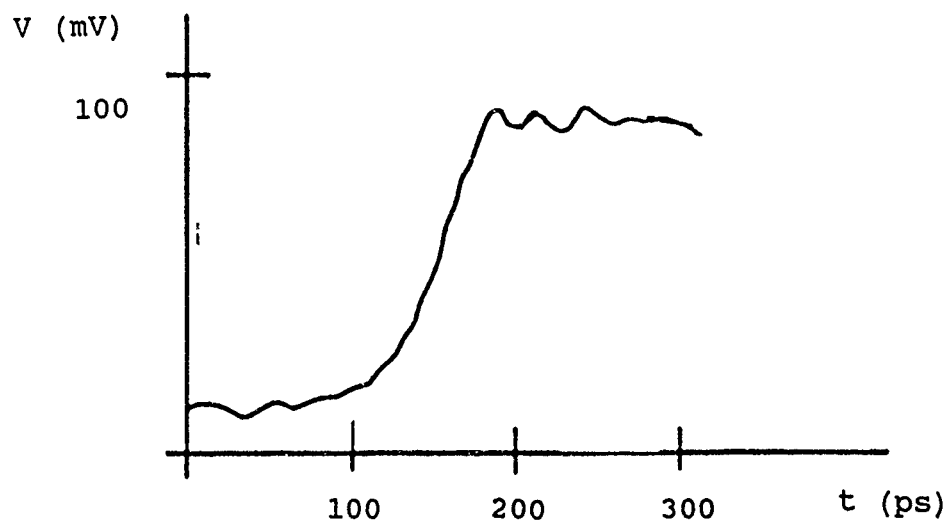


Fig. 13 Output voltage waveform for SFFT with junction

An output risetime of approximately 100 ps with an output voltage swing of about 70 mV resulted. As detailed in [10] this Tl film SFFT was then connected to a GaAs FET transistor. This arrangement yielded an output voltage swing of almost 200 mV with a 200 ps risetime.

### 9. Device stability

As anticipated, no problems were found regarding thermal cycling of NbN circuits. YBCO films required substantial care in processing and experimentation, however. Moisture condensation on the film surface must be avoided as well as excessive power dissipation in the device. Nevertheless, at least in one instance a YBCO SFFT without a passivation layer has lasted through several thermal cycles over a period of approximately 6 months. Passivation was not employed but is believed to be available from coatings with HR 100 photoresist, which was shown to withstand repeated thermal cycling. Non-recoverable damage to devices has occurred when they were biased with a current source and driven past the maximum flux-flow voltage (Fig. 14).



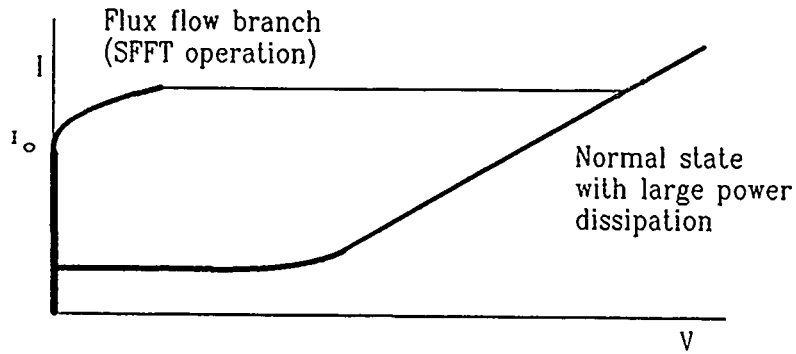


Fig. 14 Complete SFFT I-V characteristic  
 showing potential for excess power  
 dissipation due to self heating

A switch into the normal state with large associated voltages occurs in this situation. The power dissipated in the device then exceeds the damage level. Altered characteristics or complete failure resulted.

### 10. SFFT applications

While the use of SFTTs as interfaces in digital electronic circuits appears to be a suitable first application of this device, other configurations also were explored. For example, it was demonstrated that two devices connected as shown in Fig. 15 function as the equivalent of a dual gate field effect transistor [11].

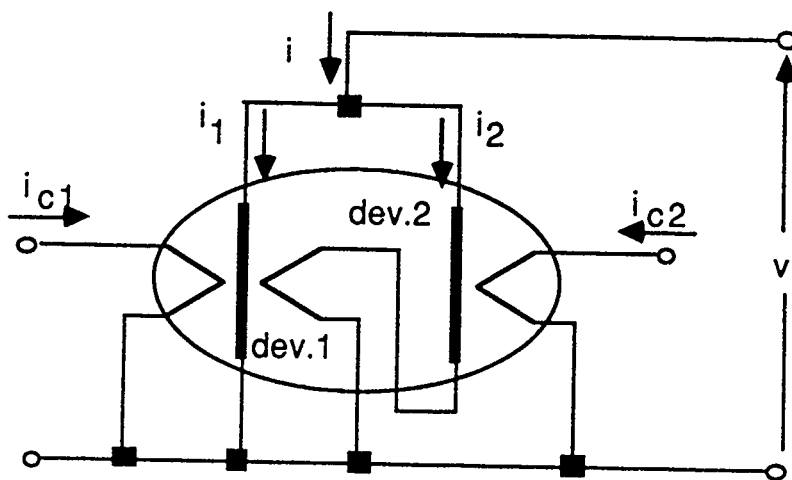


Fig. 15 Dual control SFFT

In this arrangement, one device controls the gain of the other. Mixers and gain control stages that operate well into the microwave regime should become possible.

An arrangement of several SFFTs in a distributed amplifier should provide a large gain over a wide frequency range. Simulations with the device architecture shown in Fig. 16 based on the measured device characteristics were carried out.

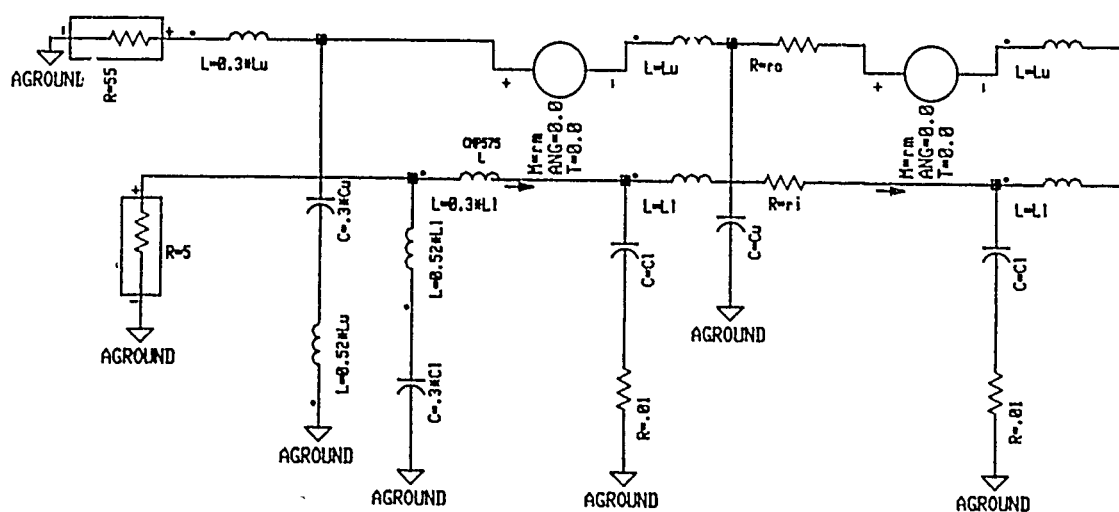


Fig. 16 Device architecture for distributed amplifier simulations

The input transmission line characteristic impedance was assumed to be 5 Ohms, a level commensurate with the typically low impedance levels of low temperature superconducting electronics circuits. The output transmission line impedance was 50 Ohms. Computer modeling resulted in the following transmission characteristics (Fig. 17).

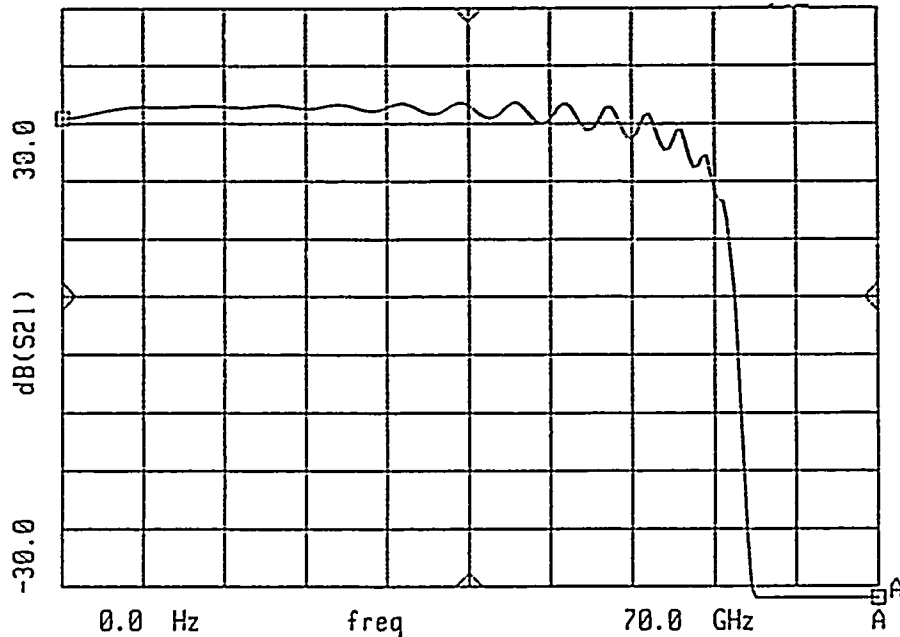


Fig. 17 Distributed SFFT amplifier simulation results

Very recently, encouraging results have been reported from an amplifier circuit fabricated with Tl films at Sandia National Laboratories.

Other applications may well emerge. Phase shifting should be possible with SFFT's and multiple wafers containing large arrays of devices might one day be used as persistent current switches in superconducting energy storage applications, for example.

## 11. Conclusions

We have successfully demonstrated the prototype fabrication of a device based on the flow of magnetic flux in multiple parallel links of a weak superconducting film. Fabrication of these superconducting flux flow transistors (SFFT) was performed with both, niobium nitride and YBCO "high temperature" superconductor thin films. Of the two, the YBCO devices far outperformed the NbN circuits, likely due to the relatively weak pinning of flux in the YBCO films. Prototype interface circuit operation of niobium-lead Josephson junction connected to a SFFT was demonstrated. Models for computer simulation were established. Additional potential applications for the SFFT device concept were identified. It has become clear, that a reduction of the concept to practice will require the development of improved fabrication and device characterization techniques. The work reported here drew on multiple resources in addition to this contract. Assistance was also provided through internal resources of HYPRES, Inc. and from on-going programs at the University of Wisconsin, Madison and Sandia National Laboratories.

## 12. References

- [1] K.K. Likharev, "Vortex Motion and the Josephson Effect in Superconducting Thin Bridges," Phys. JETP, Vol. 34, April 1972.
  
- [2] G.K.G. Hohenwarter, J.S. Martens, D.P. McGinnis, J.B. Beyer and J.E. Nordman, "Single Superconducting Thin-film Devices for Applications in High  $T_c$  Materials Circuits," IEEE Trans. on Magnetics, Vol. 25, No. 2, March 1989.
  
- [3] G.K.G. Hohenwarter, J.S. Martens and D.S. Ginley, "Characteristics of Superconducting Flux-Flow Transistors," IEEE Trans. on Mag., Vol. 27, No. 2, p. 3297, March 1991.
  
- [4] HYPRES, Inc. internal report, "Standard Process Design Rules for Fabricating Superconducting Integrated Circuits," (1986).
  
- [5] L. (Rao) Madhavrao, E.K. Track, R.E. Drake, R. Patt, G.K.G. Hohenwarter and M. Radparvar, "Microstructural, Transport, and RF Properties of Multilayer-Deposited YBCO Films," IEEE Trans. on Mag., Vol. 27, No. 2, p. 1402, March 1991.
  
- [6] J.S. Martens, private communication.